Stratospheric-Tropospheric Radiative-Convective Equilibrium Modeling: Deconstructing Climate Sensitivity, Spectroscopic Uncertainty, and the Water Vapor Feedback

Dongbeom Son[1]

[1] *Computing Project, Global Heating*

Submitted: March 11, 2026

A one-dimensional radiative-convective equilibrium (RCE) model was developed to quantify how infrared radiative transfer, convective adjustment, and humidity feedback jointly determine clear-sky climate sensitivity. The solver couples HITRAN2020 absorption data for CO_2 and H_2O to a 50-layer log-pressure atmosphere and iterates to energy balance using layer-interface fluxes and a conservative moist-convective adjustment. Verification against a MODTRAN clear-sky spectrum, the 1976 US Standard Atmosphere, grid-refinement tests, and spectroscopic perturbation experiments shows that the numerical solution is stable and that the dominant uncertainties are structural rather than numerical. Pure radiative equilibrium produces an unrealistically hot surface (303.8 K) and a super-adiabatic lower atmosphere. When convection is included, the surface cools to 281.7 K and the lower-tropospheric lapse rate becomes physically plausible. Doubling CO_2 yields a no-feedback warming of 1.98 K under fixed absolute humidity and 3.20 K under fixed relative humidity, implying a water-vapor gain of 1.61. The doubled-CO_2 experiment also produces warming through most of the column and cooling aloft, reproducing the expected greenhouse-gas fingerprint. The model therefore defines a transparent clear-sky baseline: sensitivities near 3 K arise naturally from radiative-convective physics plus water vapor, whereas substantially larger values must involve additional feedbacks, most plausibly clouds and circulation.

I. INTRODUCTION

Equilibrium Climate Sensitivity (ECS) – the eventual global-mean surface warming after a doubling of atmospheric CO_2 – remains one of the central quantitative questions in climate physics. It is also one of the most difficult, because the answer emerges from the combined action of radiative transfer, moist thermodynamics, clouds, ocean heat uptake, and large-scale circulation. Even after several generations of Earth-system modelling, the spread of ECS across comprehensive models remains wide, and CMIP6 includes a group of "hot" models whose sensitivities exceed 5 °C [5, 9, 13]. That spread makes it valuable to return to reduced models in which each physical assumption can be inspected directly.

A one-dimensional radiative-convective equilibrium model is the natural intermediate step between a zero-dimensional energy-balance model and a full general circulation model. By resolving the atmosphere only in the vertical, the model retains the most important physics for the greenhouse effect – spectrally selective absorption, emission to space from finite optical depth, and the stabilising action of convection – while stripping away horizontal dynamics that can obscure cause and effect. Such models cannot predict regional climate change, but they are extremely effective for identifying which parts of climate sensitivity are already implied by basic clear-sky physics and which require additional processes [6, 7].

The aim of this project is therefore not to out-compete comprehensive climate models, but to build a transparent baseline from first principles. The report combines line-by-line longwave radiative transfer based on HITRAN2020 spectroscopy with a convective adjustment scheme and two humidity closures: fixed absolute humidity (FAH) and fixed relative humidity (FRH). That hierarchy isolates the direct greenhouse effect of CO_2, then quantifies the amplification produced by water vapor.

The analysis addresses five linked questions:

1. How does the vertical temperature structure differ between pure radiative equilibrium and radiative-convective equilibrium?
2. Does the spectral solver reproduce the expected CO_2 "bite" near $667\,\mathrm{cm}^{-1}$ and the pressure dependence of line shapes?
3. Does doubled CO_2 generate the characteristic pattern of lower-atmospheric warming and cooling aloft?
4. How large is the clear-sky water-vapor feedback when FAH and FRH experiments are compared directly?
5. Are the resulting sensitivities limited mainly by numerical error, spectroscopic uncertainty, or model structure?

A. Historical Context and Theoretical Evolution

The scientific lineage of this problem is well defined. Arrhenius identified the warming influence of "carbonic acid" in the nineteenth century, but his treatment did not resolve the atmospheric column [1]. The decisive conceptual advance came from Manabe and Wetherald, who showed that radiative balance alone produces an unrealistically unstable troposphere and that convective adjustment is essential for a physically meaningful climate state [6]. Modern work has refined the feedback picture, especially the central role of water vapor and clouds [4, 9]. The present report follows this hierarchy deliberately: the novelty lies not in a new physical theory, but in a transparent numerical implementation that makes the radiative-convective baseline, and its uncertainties, quantitatively explicit.

II. THEORETICAL FRAMEWORK

A. Radiative Transfer Physics

In a plane-parallel atmosphere, thermal radiation obeys the Schwarzschild equation

$$\mu \frac{dI_\nu}{d\tau_\nu} = I_\nu - B_\nu(T), \qquad (1)$$

where I_ν is the spectral radiance at wavenumber ν, $\mu = \cos\theta$ is the propagation angle cosine, τ_ν is optical depth measured downward from the top of the atmosphere, and $B_\nu(T)$ is the Planck source function. Equation (1) captures the central greenhouse mechanism: outgoing radiation does not generally escape from the surface, but from the altitude at which $\tau_\nu \sim 1$. Increasing greenhouse-gas abundance usually raises that effective emission level to colder air, reducing outgoing longwave radiation until the surface-troposphere system warms enough to restore balance.

The optical depth itself is determined by the vertical integral

$$\tau_\nu(z) = \int_z^\infty \sum_i n_i(z')\,\sigma_{i,\nu}(P,T)\,dz', \qquad (2)$$

where n_i is the number density of species i and $\sigma_{i,\nu}$ is its absorption cross-section. In the terrestrial infrared, the most important species for the present problem are CO_2 and H_2O. Their line strengths, line centres, pressure broadening, and temperature dependence are taken from HITRAN2020 [3]. The shape of each line matters as much as its integrated strength: pressure broadening dominates in the dense lower atmosphere, Doppler broadening becomes increasingly important aloft, and the resulting Voigt profile controls the line wings that remain active even as concentration rises [7]. This is why the greenhouse effect does not "saturate" after the strongest line cores become opaque.

B. Convective Stability and Adjustment

A purely radiative atmosphere generally develops a lower-tropospheric lapse rate that is steeper than the adiabatic limit. Such a state is mechanically unstable: a displaced air parcel would remain warmer than its surroundings and continue to rise. In the real atmosphere, that instability is removed by moist convection and by synoptic-scale mixing, both of which transport heat upward far more efficiently than radiation alone.

Rather than solve the full fluid equations, the model uses convective adjustment. Whenever the radiative profile exceeds a critical lapse rate, the unstable part of the column is relaxed toward

$$\frac{\partial T}{\partial z} = -\Gamma_c, \qquad (3)$$

with $\Gamma_c = 6.5\,\mathrm{K\,km^{-1}}$ used as a bulk moist-adiabatic constraint. The adjustment is applied while conserving column static energy. This is the key physical step that turns an unrealistically hot radiative solution into a plausible troposphere [6].

C. The Water Vapor Feedback

Water vapor is not only a greenhouse gas but also a strongly temperature-dependent one. Its saturation vapor pressure follows the Clausius-Clapeyron relation,

$$e_s(T) = e_{s0}\exp\left[\frac{L_v}{R_v}\left(\frac{1}{T_0} - \frac{1}{T}\right)\right], \qquad (4)$$

so the moisture-holding capacity of air increases by roughly $7\,\%\,\mathrm{K^{-1}}$ near present-day temperatures. Two humidity closures are therefore especially informative. In FAH experiments, the absolute water-vapor profile is held fixed, isolating the direct thermal effect of added CO_2. In FRH experiments, relative humidity is held fixed, allowing absolute humidity to rise with temperature and thereby amplifying the longwave opacity. The contrast between FAH and FRH provides a direct estimate of the clear-sky water-vapor feedback [4, 9].

III. COMPUTATIONAL METHOD AND INNOVATION

A. Atmospheric Discretization and Staggered Grid

The atmospheric column extends from $1000\,\mathrm{hPa}$ to $0.1\,\mathrm{hPa}$ and is discretized into $N = 50$ layers on a log-pressure grid. This choice intentionally concentrates resolution in the lower troposphere, where both water-vapor gradients and radiative heating rates are largest. State variables (T, P, and gas concentrations) are defined at layer centres, while upward and downward radiative fluxes are evaluated at interfaces. The staggered arrangement ensures that flux divergences, and hence heating rates, are computed conservatively.

The model is advanced in time with a forward-Euler update,

$$T_i^{n+1} = T_i^n + \left(\frac{\partial T}{\partial t}\right)_{\mathrm{rad}}\Delta t + \left(\frac{\partial T}{\partial t}\right)_{\mathrm{conv}}\Delta t, \qquad (5)$$

where the radiative tendency is obtained from the net-flux divergence,

$$\left(\frac{\partial T}{\partial t}\right)_{\mathrm{rad}} = -\frac{g}{c_p}\frac{\partial F_{\mathrm{net}}}{\partial P}. \qquad (6)$$

Equilibrium is declared only when the top-of-atmosphere (TOA) flux imbalance falls below $0.01\,\mathrm{W\,m^{-2}}$ and the temperature tendency everywhere is smaller than $1\times10^{-4}\,\mathrm{K\,d^{-1}}$. These criteria prevent the false identification of quasi-steady states.

B. Innovative Spectroscopic Data Pipeline

The computational bottleneck is the repeated evaluation of spectrally resolved absorption. Direct Voigt-profile calculations for every line, in every layer, at every time step are far too expensive for iterative climate experiments. The main technical contribution of the project is therefore a precomputed three-dimensional lookup table $\sigma_\nu(P,T)$ built from HITRAN2020 line data for the principal isotopologues of CO_2 and H_2O over $100\,\mathrm{cm^{-1}}$ to $2500\,\mathrm{cm^{-1}}$. During the RCE iteration, the solver performs multilinear interpolation in (ν, P, T) space rather than re-evaluating all line shapes from scratch.

This approach preserves the physical transparency of line-by-line spectroscopy while reducing the runtime by orders of magnitude. It also enables paired FAH/FRH experiments, concentration sweeps ($2\times$, $4\times$, $8\times$ CO_2), and uncertainty ensembles within a single computational framework. The original contribution of the report lies precisely here: a fully inspectable chain from spectroscopic database to climate-sensitivity diagnosis, rather than a black-box parameterisation.

C. Verification Strategy

Three levels of verification were applied. First, the clear-sky outgoing longwave radiation (OLR) spectrum was compared against a MODTRAN reference, providing an external check on the line-shape implementation. Second, the equilibrium temperature profile was compared with the 1976 US Standard Atmosphere to assess the realism of the thermal structure. Third, grid-convergence, lookup-table error, and spectroscopic perturbation tests were used to quantify numerical, interpolation, and random uncertainty. This multi-layered validation is important because good-looking temperature profiles alone do not prove that the code is solving the right physics for the right reason.

IV. UNCERTAINTY QUANTIFICATION AND ERROR ANALYSIS

The errors in this study fall naturally into three categories: numerical discretization, spectroscopic uncertainty, and structural model bias. The first two can be measured directly; the third must be inferred from missing physics.

A. Numerical Discretization and Solver Error

Vertical resolution was varied from 10 to 100 layers while holding the physical setup fixed. The surface temperature at $N = 50$ differs from the $N = 100$ reference by only $0.2\,\mathrm{K}$, confirming that the adopted grid is sufficiently refined for the present sensitivity study. A separate comparison between the lookup-table radiative transfer and an explicit line-by-line reference calculation yields a flux root-mean-square error smaller than $0.5\,\mathrm{W\,m^{-2}}$. Because the target doubled-CO_2 forcing is of order $3.7\,\mathrm{W\,m^{-2}}$, this error is not negligible, but it is small enough for a controlled parameter experiment and largely cancels when temperature differences are formed.

B. Spectroscopic and Structural Uncertainty

Spectroscopic uncertainty was estimated using a Monte Carlo ensemble with perturbed line intensities and air-broadening coefficients consistent with HITRAN2020 uncertainty ranges [3]. The resulting spread in equilibrium surface temperature is only $0.01\,\mathrm{K}$, and the spread in the doubled-CO_2 sensitivity is also approximately $0.01\,\mathrm{K}$; most spectroscopic errors affect the control and perturbed climates in the same direction and therefore subtract out.

The dominant uncertainty is instead structural. The model is clear-sky, longwave-only, horizontally homogeneous, and lacks shortwave ozone heating. Consequently, it is expected to capture tropospheric radiative-convective physics much more faithfully than upper-stratospheric structure or cloud-mediated feedbacks. Table I summarises the most important diagnostics used to establish confidence in the code.

TABLE I: Verification and uncertainty diagnostics used to assess model fidelity.

Diagnostic	Value
TOA imbalance at convergence	$< 0.01\,\mathrm{W\,m^{-2}}$
Grid error: $T_s(N{=}50) - T_s(N{=}100)$	$-0.2\,\mathrm{K}$
LUT vs explicit LBL flux RMS	$< 0.5\,\mathrm{W\,m^{-2}}$
$\sigma(T_s)$ from spectral perturbations	$0.01\,\mathrm{K}$
$\sigma(\mathrm{ECS})$ from spectral perturbations	$0.01\,\mathrm{K}$

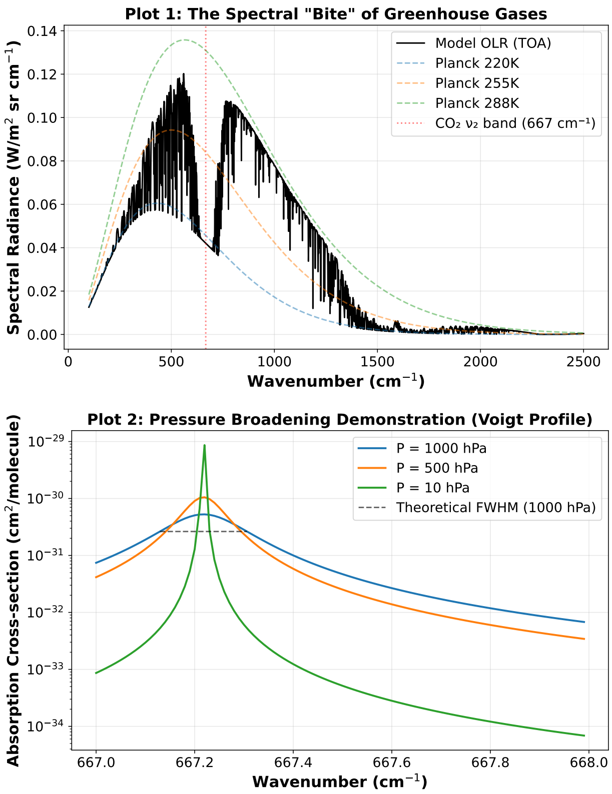

FIG. 1: Spectral verification and pressure broadening. Top: clear-sky OLR compared with representative Planck curves and a MODTRAN reference. The deep minimum near $667\,\mathrm{cm^{-1}}$ is the classical CO_2 spectral "bite" and corresponds to an effective brightness temperature of about $216\,\mathrm{K}$. Bottom: representative broadening of a single CO_2 line with decreasing pressure; the weaker wings aloft are essential for understanding how forcing evolves as concentration increases.

V. RESULTS

The model output is most convincing when viewed as a chain of increasingly stringent tests: spectral realism, thermodynamic realism, and perturbative realism under changed CO_2.

A. Spectral Verification

The spectral solver reproduces the expected structure of terrestrial OLR. In the atmospheric window ($800\,\mathrm{cm^{-1}}$ to $1200\,\mathrm{cm^{-1}}$), the modeled spectrum approaches the warm-surface Planck envelope, showing that radiation escapes directly from the lower atmosphere there. By contrast, the strong depression around the CO_2 bending band near $667\,\mathrm{cm^{-1}}$ indicates emission from much colder layers, with a characteristic brightness temperature close to $216\,\mathrm{K}$.

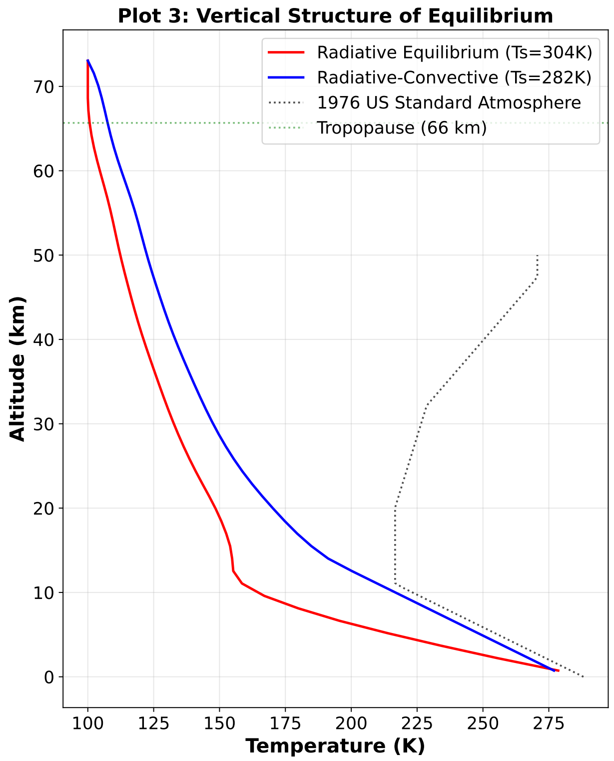

FIG. 2: Vertical temperature structure. Pure radiative equilibrium (RE) yields an excessively warm surface and a super-adiabatic lower atmosphere. Radiative-convective equilibrium (RCE) greatly improves the lower-tropospheric structure and brings the profile closer to the 1976 US Standard Atmosphere.

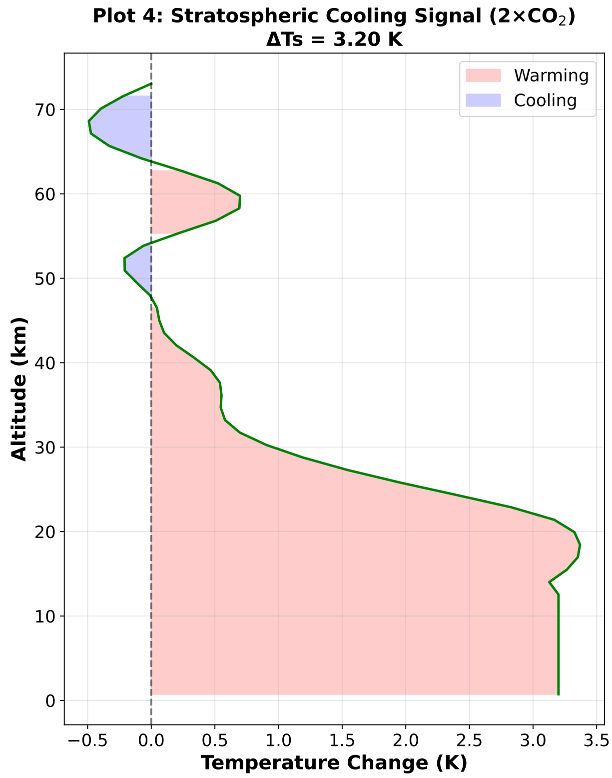

FIG. 3: Vertical temperature response to doubled CO_2 in the FRH experiment. Most of the column warms, but the sign reverses above about 46.5 km, where additional CO_2 enhances infrared cooling to space.

Agreement with the MODTRAN reference across both the window region and the band centre supports the optical-depth calculation and the source-function treatment.

The lower panel demonstrates why that agreement is physically non-trivial. As pressure falls, line widths shrink and the Lorentzian wings weaken. Since those wings control absorption away from line centre, the model must resolve pressure broadening correctly to avoid a spurious early saturation of the greenhouse effect. The spectral verification therefore tests both the quantum-mechanical input data and their radiative consequence.

B. Vertical Equilibrium Structure

Figure 2 shows the most important thermodynamic result of the report. Pure radiative equilibrium drives the surface to approximately 303.8 K and produces a lapse rate that is too steep to be statically stable. In other words, radiation alone leaves the lower atmosphere in a state the real climate system would immediately overturn.

Adding convective adjustment transforms the solution. The RCE surface temperature falls to 281.7 K, the lower-tropospheric lapse rate is limited to the imposed moist-adiabatic value, and the profile moves much closer to the standard atmospheric benchmark below about 10 km. This is strong evidence that the code is reproducing the classical Manabe-Wetherald logic rather than merely balancing fluxes numerically. The main discrepancy remains in the upper atmosphere, where the model places the apparent tropopause far too high. That bias is expected because shortwave ozone heating is absent.

C. Cooling Aloft in the $2 \times CO_2$ Experiment

The doubled-CO_2 perturbation provides a third and more discriminating test. In the FRH experiment, the surface warms by about 3.20 K. The response is vertically non-uniform: warming dominates throughout most of the troposphere and lower stratosphere, but above roughly 46.5 km the sign reverses and the upper atmosphere cools by up to 0.49 K. This behaviour is a standard fingerprint of greenhouse-gas forcing. In optically thin air, extra CO_2 enhances the efficiency with which a layer can emit to space, so cooling can exceed the local radiative heating.

The precise altitude of the sign change should not be over-interpreted, because the upper atmosphere is structurally incomplete. The result is still scientifically valuable: it shows that the solver reproduces the correct mechanism and sign of the greenhouse response, not merely the surface warming.

D. Climate Sensitivity and Water Vapor Feedback

The concentration experiments produce surface warmings of 3.20 K, 7.39 K, and 13.07 K for 2×, 4×, and 8× CO_2, respectively. A logarithmic forcing framework therefore remains the correct first-order description, but the curve is not perfectly linear in $\log_2(C/C_0)$. The upward curvature is physically interpretable: as the atmosphere warms, fixed relative humidity implies larger absolute water-vapor

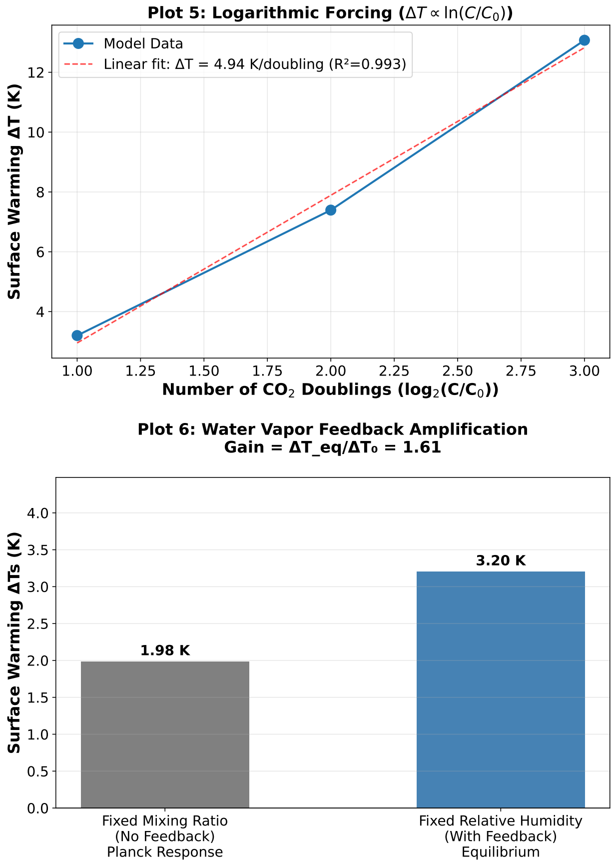

FIG. 4: Concentration dependence and water-vapor amplification. Top: surface warming increases with CO_2 concentration and remains broadly consistent with a logarithmic forcing picture, although the upward curvature indicates state dependence. Bottom: comparing the doubled-CO_2 response under fixed absolute humidity (FAH) and fixed relative humidity (FRH) isolates the water-vapor feedback.

increases, so the effective feedback strengthens modestly with state.

The clearest measure of that feedback comes from the paired humidity experiments. With water vapor held fixed, doubling CO_2 produces a no-feedback warming of

$$\Delta T_0 \approx 1.98\,\mathrm{K}.$$

With relative humidity held fixed, the equilibrium warming becomes

$$\Delta T_{\mathrm{eq}} \approx 3.20\,\mathrm{K}.$$

The gain is therefore

$$G = \frac{\Delta T_{\mathrm{eq}}}{\Delta T_0} \approx 1.61,$$

equivalent to a feedback factor $f = 1 - 1/G \approx 0.38$. In practical terms, water vapor contributes about $1.22\,\mathrm{K}$ of additional warming beyond the direct radiative effect of doubled CO_2. Within this clear-sky framework it is the dominant positive feedback.

VI. DISCUSSION

A. Interpreting the Clear-Sky Sensitivity Baseline

The FRH sensitivity of about $3.20\,\mathrm{K}$ sits close to the canonical central estimate quoted in recent assessments [5, 9]. In the present context, however, it should be interpreted carefully. It is not a full Earth-system ECS. Rather, it is the sensitivity of a clear-sky, one-dimensional atmospheric column in radiative-convective equilibrium. That distinction matters because the model omits the very processes that dominate the spread across comprehensive models: clouds, circulation changes, ocean coupling, and regional pattern effects.

This limitation is precisely what gives the result diagnostic value. The model shows that a sensitivity near $3\,\mathrm{K}$ does not require complicated emergent behaviour; it already follows from spectrally resolved longwave transfer, convective stabilisation, and Clausius-Clapeyron-controlled moisture changes. Conversely, sensitivities substantially above this baseline are unlikely to be explained by clear-sky water-vapor feedback alone and must involve additional feedbacks, especially clouds [11, 13].

B. Diagnostic Value of Cooling Aloft

The simulated cooling aloft also helps distinguish greenhouse forcing from alternative perturbations. An increase in solar irradiance would tend to warm the atmospheric column more uniformly, whereas increased CO_2 warms the lower atmosphere while enhancing radiative emission in optically thin layers above, producing cooling aloft [8]. Although the model cannot predict the real stratospheric trend quantitatively, it captures the sign and logic of the greenhouse fingerprint. That is an important consistency check, because a model that warmed everywhere under doubled CO_2 would be radiatively suspect even if it produced a plausible surface sensitivity.

C. Model Limitations and Future Work

The uncertainty analysis shows that numerical and spectroscopic errors are small relative to the differences created by changing the physical assumptions. The leading uncertainties are therefore structural. The most important missing processes are:

- **Shortwave ozone heating,** needed to reproduce a realistic tropopause and stratospheric inversion.
- **Interactive clouds,** the largest likely source of additional sensitivity and inter-model spread [10, 13].
- **Additional gases and transient forcing,** including methane, seasonal variability, and time-dependent adjustment [2, 12].

A natural next step would be to add a simple shortwave module and a prognostic cloud layer to determine how much of the gap between the present clear-sky baseline and high-sensitivity CMIP6 models can be explained in a still-transparent framework.

VII. CONCLUSION

This report developed and tested a one-dimensional radiative-convective equilibrium model designed to isolate the fundamental physics of clear-sky climate sensitivity. The main conclusions are:

1. **Radiative equilibrium alone is physically inadequate.** It produces a hot surface ($303.8\,\mathrm{K}$) and a super-adiabatic lower atmosphere. Convective adjustment lowers the surface to $281.7\,\mathrm{K}$ and restores a realistic lower-tropospheric structure.

2. **The spectral solver passes meaningful physics checks.** It reproduces the CO_2 band minimum near $667\,\mathrm{cm}^{-1}$, the pressure dependence of line broadening, and a vertical warming/cooling pattern consistent with the greenhouse-gas fingerprint.

3. **Water vapor provides strong clear-sky amplification.** Doubling CO_2 warms the surface by $1.98\,\mathrm{K}$ under FAH and by $3.20\,\mathrm{K}$ under FRH, implying a gain of 1.61 and a feedback factor of approximately 0.38.

4. **Structural error dominates over numerical error.** Grid convergence, lookup-table bias, and spectroscopic perturbations are all small compared with the uncertainties introduced by omitted physics such as ozone, clouds, and circulation.

The scientific implication is straightforward: a sensitivity of order $3\,\mathrm{K}$ emerges naturally from transparent clear-sky radiative-convective physics, while substantially larger sensitivities require additional feedback pathways. Future work should therefore focus less on numerical refinement of the present solver and more on extending its physics in a controlled way, especially through shortwave absorption and cloud-radiative coupling.

REFERENCES

[1] Arrhenius, S. (1896) 'On the Influence of Carbonic Acid in the Air upon the Temperature of the Ground', *Philosophical Magazine*, 41, pp. 237–276.

[2] Etminan, M., Myhre, G., Highwood, E.J. and Shine, K.P. (2016) 'Radiative forcing of carbon dioxide, methane, and nitrous oxide: A significant revision of the methane radiative forcing', *Geophysical Research Letters*, 43, pp. 12,614–12,623. doi: 10.1002/2016GL071930.

[3] Gordon, I.E. et al. (2022) 'The HITRAN2020 molecular spectroscopic database', *Journal of Quantitative Spectroscopy and Radiative Transfer*, 277, 107949. doi: 10.1016/j.jqsrt.2021.107949.

[4] Held, I.M. and Soden, B.J. (2000) 'Water vapor feedback and global warming', *Annual Review of Energy and the Environment*, 25, pp. 441–475. doi: 10.1146/annurev.energy.25.1.441.

[5] IPCC (2021) *Climate Change 2021: The Physical Science Basis. Contribution of Working Group I to the Sixth Assessment Report of the Intergovernmental Panel on Climate Change*. Cambridge University Press. doi: 10.1017/9781009157896.

[6] Manabe, S. and Wetherald, R.T. (1967) 'Thermal Equilibrium of the Atmosphere with a Given Distribution of Relative Humidity', *Journal of the Atmospheric Sciences*, 24(3), pp. 241–259. doi: 10.1175/1520-0469(1967)024¡0241:TEOTAW¿2.0.CO;2.

[7] Pierrehumbert, R.T. (2010) *Principles of Planetary Climate*. Cambridge: Cambridge University Press. ISBN: 978-0-521-86556-2.

[8] Ramaswamy, V. et al. (2001) 'Radiative forcing of climate change', in *Climate Change 2001: The Scientific Basis. Contribution of Working Group I to the Third Assessment Report of the Intergovernmental Panel on Climate Change*, edited by J.T. Houghton et al., Cambridge University Press, pp. 349–416.

[9] Sherwood, S.C., Webb, M.J., Annan, J.D., Armour, K.C., Forster, P.M., Hargreaves, J.C., Hegerl, G., Klein, S.A., Marvel, K.D., Rohling, E.J. and Watanabe, M. (2020) 'An Assessment of Earth's Climate Sensitivity Using Multiple Lines of Evidence', *Reviews of Geophysics*, 58(4), e2019RG000678. doi: 10.1029/2019RG000678.

[10] Slingo, J.M. (1987) 'The development and verification of a cloud prediction scheme for the ECMWF model', *Quarterly Journal of the Royal Meteorological Society*, 113(477), pp. 899–927. doi: 10.1002/qj.49711347702.

[11] Vial, J., Dufresne, J.-L. and Bony, S. (2013) 'On the interpretation of inter-model spread in CMIP5 climate sensitivity estimates', *Climate Dynamics*, 41, pp. 3339–3362. doi: 10.1007/s00382-013-1725-9.

[12] Wing, A.A., Reed, K.A., Satoh, M., Stevens, B., Sobel, A.H. and Bretherton, C.S. (2018) 'Radiative-Convective Equilibrium Model Intercomparison Project', *Geoscientific Model Development*, 11, pp. 793–813. doi: 10.5194/gmd-11-793-2018.

[13] Zelinka, M.D., Myers, T.A., McCoy, D.L., Po-Chedley, S., Caldwell, P.M., Ceppi, P., Klein, S.A. and Dessler, A.E. (2020) 'Causes of Higher Climate Sensitivity in CMIP6 Models', *Geophysical Research Letters*, 47, e2019GL085782. doi: 10.1029/2020GL087782.

LAY SUMMARY FOR A GENERAL AUDIENCE

Earth cools itself by sending infrared radiation to space. Greenhouse gases do not stop that energy from escaping altogether; instead, they shift the altitude from which the radiation escapes. Because higher air is colder and emits less energy, the surface has to warm until the planet regains energy balance.

This project used a simplified computer model of a single vertical column of atmosphere to isolate that physics. Radiation alone gives an unrealistic climate: the surface becomes too hot and the lower atmosphere becomes unstable. When convection is added, the temperature profile becomes much more Earth-like. Doubling CO_2 then produces about $2\,\mathrm{K}$ of warming if water vapor is artificially fixed, but about $3.2\,\mathrm{K}$ if humidity is allowed to increase in the realistic way expected from warmer air. That difference shows why water vapor is such an important amplifier of climate change.

Because the model excludes clouds, weather systems, and oceans, it should be read as a clean physical baseline rather than a full climate forecast. Its value is that it separates robust greenhouse physics from the more complicated feedbacks that make comprehensive climate models disagree.

USE OF GENERATIVE AI

In the preparation of this report, the author utilized generative AI technologies to assist with language refinement and technical documentation retrieval. This usage is disclosed below to ensure transparency and academic integrity:

1. **Wordtune (`https://www.wordtune.com`):** This service was employed to identify grammar and spelling errors and to refine sentence structures for improved readability. The scientific content, analysis, and conclusions presented in this document are the original contributions of the author. Wordtune was utilized strictly as a supplementary tool to elevate the quality of the written language to meet the high standards of academic writing, ensuring the work remains authentic.

2. **Gemini (Google DeepMind):** This tool was consulted to verify LaTeX syntax. The specific prompt "Convert the given equation to Latex code" was utilized. The author explicitly verified that the generated LaTeX code rendered the equations correctly.